Journal of The Electrochemical Society, **148** (2) C88-C94 (2001)
0013-4651/2001/148(2)/C88/7/$7.00 © The Electrochemical Society, Inc.

Electrodeposition of Silver-Aluminum Alloys from a Room-Temperature Chloroaluminate Molten Salt

Qun Zhu,[a,*] Charles L. Hussey,[a,,z] and Gery R. Stafford[b,**]**

[a]*Department of Chemistry and Biochemistry, The University of Mississippi, University, Mississippi 38677, USA*
[b]*National Institute of Standards and Technology, Materials Science and Engineering Laboratory, Gaithersburg, Maryland 20899, USA*

The electrodeposition of silver-aluminum alloys was investigated at platinum and tungsten electrodes in the Lewis acidic aluminum chloride-1-ethyl-3-methylimidazolium chloride ($AlCl_3$-EtMeImCl) molten salt containing electrogenerated silver(I) at 25°C. Sampled-current voltammetry indicated that it is possible to electrodeposit Ag-Al alloys at potentials positive of that where the bulk deposition of aluminum is normally observed (~0 V). The aluminum content of these alloys varied with the applied potential and displayed an inverse dependence on the silver(I) concentration, indicating that the alloy formation process was kinetically limited. Experiments conducted in melts with different compositions revealed that at a fixed potential and silver(I) concentration, the atomic fraction of aluminum in the alloy is virtually independent of the melt composition. At high concentrations, silver(I) adsorbs on platinum and tungsten, but this process is inhibited by the addition of benzene. The adsorption process does not appear to affect the codeposition of aluminum with silver. X-ray diffraction analysis of bulk Ag-Al alloy electrodeposits prepared in melt containing benzene as a cosolvent indicated the presence of both face-centered cubic Ag and hexagonal close-packed δ-Ag_2Al.
 [DOI: 10.1149/1.1339863]

Manuscript submitted July 10, 2000; revised manuscript received October 12, 2000.

Transition metal-aluminum alloys are technologically important because of their corrosion resistance and, in some cases, their interesting magnetic properties. Electrodeposition is a useful method for producing alloy films with uniform thickness, small grain size, and homogeneous composition. Chloroaluminate molten salts such as $AlCl_3$-NaCl and related lower melting chloroaluminates based on quaternary ammonium chloride salts such as 1-(1-butyl)pyridinium chloride (BuPyCl) or 1-ethyl-3-methylimidazolium chloride (EtMeImCl) have been shown to be useful solvents for the electrodeposition of these alloys. The attractiveness of chloroaluminate melts stems from the fact that these ionic solvents are concentrated reservoirs of easily reducible aluminum-containing species such as $Al_2Cl_7^-$. Some of the aluminum alloys that have been electrodeposited from these melts include Co-Al,[1,2] Cr-Al,[3,4] Cu-Al,[5] Fe-Al,[6] Mn-Al,[7,8] and Ni-Al.[9,10] The electrodeposition of Cr-Al and Mn-Al takes place at potentials proximate to the equilibrium potential of the Al(III)/Al couple, whereas the codeposition of Al with Co, Cu, Fe, and Ni is observed at potentials considerably positive of that at which the deposition of bulk aluminum is normally observed. The latter phenomenon in which aluminum codeposits with the transition metal at ''underpotentials'' has been ascribed to the free energy gain resulting from alloy formation.[9]

The $AlCl_3$-EtMeImCl molten salt is especially attractive for the electrodeposition of transition metal-aluminum alloys because it has a very low melting point over a wide range of compositions, high intrinsic electrical conductivity at room temperature, and a negligible vapor pressure due to the escape of $AlCl_3$ and/or Al_2Cl_6.[11] Recent studies in our laboratory have revealed that aluminum electrodeposits with silver during the reduction of silver(I) in acidic $AlCl_3$-EtMeImCl to produce Ag-Al alloys. In this article, we describe the effects of melt composition, applied potential, silver(I) concentration, electrode material, and the addition of a cosolvent (benzene) on the Ag-Al electrodeposition process. The electrodeposition of Ag-Al alloy was first reported by Blue and Mathers[12] during an investigation of aluminum deposition from a benzene-xylene bath containing dissolved aluminum bromide, aluminum chloride, ethyl bromide, and silver chloride.

Experimental

Chemicals.—The methods used to prepare the EtMeImCl salt by reacting ethyl chloride and 1-methylimidazole (Aldrich, 99%) and to purify the salt by recrystallization were identical to those described previously.[13] Aluminum chloride (Fluka, puriss) was sublimed under vacuum a minimum of three times before use. The molten salt obtained by combining $AlCl_3$ and EtMeImCl was purified by constant-current electrolysis between aluminum electrodes (Alfa/Aesar, 99.9965%), filtered through a medium porosity glass frit to remove any aluminum debris that may have detached from the cathode during electrolysis, and evacuated to 1×10^{-4} Torr to remove the last traces of HCl.[14] The resulting product was water-clear and displayed no reduction waves due to proton impurities when investigated with cyclic voltammetry using a platinum electrode. Throughout this article, the melt composition is described in terms of the percent mole fraction (mol %) of each component of the $AlCl_3$-EtMeImCl mixture. Benzene (Aldrich, HPLC grade) was distilled from potassium hydride and stored over molecular sieves in the glove box until needed.

Instrumentation.—All experiments were conducted inside a dry nitrogen-filled glove box. The method used to estimate the moisture and oxygen content of the glove box atmosphere has been described.[15] Chronoamperometry, controlled-current and controlled-potential coulometry, and cyclic-staircase voltammetry experiments were carried out with an EG&G Princeton Applied Research (EG&G PARC) model 263 potentiostat/galvanostat. The latter was connected to an IBM compatible Pentium processor-based PC through an IEEE-488 bus and was controlled by EG&G PARC model 270 Research Electrochemistry software. Controlled electrode rotation was provided by a Pine Instruments AFMSRX electrode rotator.

Cells and electrodes.—The electrochemical cells used in these investigations were identical to those employed in previous studies completed in this laboratory.[16] Silver(I) was introduced into the melt by the electrodissolution of a silver working electrode. This electrode consisted of a coil of 1.0 mm diam silver wire (Alfa, m3N). Before use, this electrode was immersed in dilute nitric acid, washed with distilled water and acetone, and dried under vacuum. During experiments involving the electrodeposition of Ag-Al alloy, the counter electrode was a silver wire coil placed directly in the bulk solution. For cyclic-staircase and sampled-current voltammetry, the working electrodes were Pine Instruments Teflon-sheathed platinum

* Electrochemical Society Student Member.
** Electrochemical Society Active Member.
z E-mail: chclh@chem1.olemiss.edu

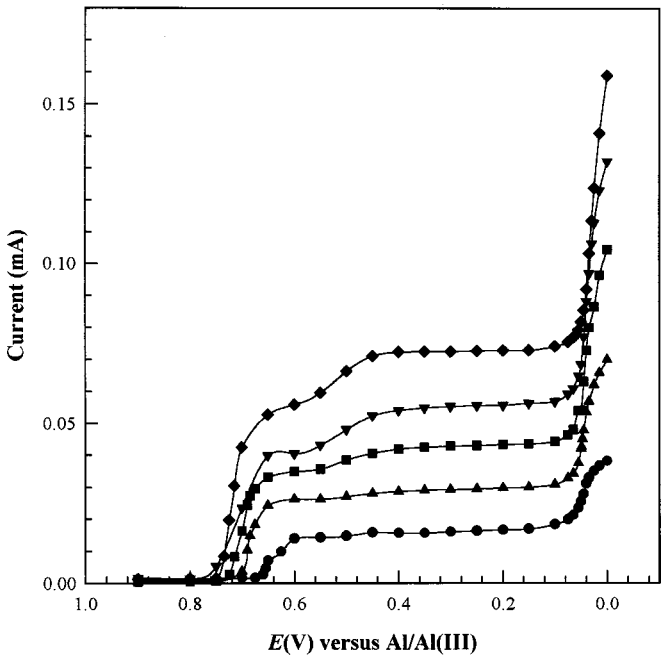

Figure 1. Sampled-current voltammograms recorded at a stationary platinum electrode in the 66.7-33.3 mol % melt. The silver(I) concentrations were (●) 5.00, (▲) 10.0, (■) 15.0, (▼) 20.0, and (♦) 25.0 mmol L^{-1}. The current was sampled at 10 s.

and tungsten rotating disk electrodes (RDE) with geometrical surface areas of 0.196 cm^2. These electrodes were polished to a mirror finish with an aqueous slurry of 0.05 μm alumina by using a Buehler Metaserve grinder/polisher, washed with distilled water, and dried under vacuum in the glove box transfer chamber before use. The reference electrode was an aluminum wire immersed in pure melt with the same composition as the bulk melt used for the electrodeposition of the Ag-Al alloy. The reference melt was isolated from the bulk melt with a fine porosity glass frit. All experiments were conducted at 25 ± 1°C.

Characterization of bulk electrodeposits.—Bulk electrodeposits were characterized by scanning electron microscopy (SEM), energy dispersive X-ray spectrometry (EDS), and X-ray diffraction (XRD) techniques using the facilities at NIST. Standardless semiquantitative analysis of EDS data taken from the as-deposited surface was used to estimate the alloy composition. The X-ray diffraction patterns were collected on a Scintag diffractometer with Cu Kα radiation. Reflections from the electrodeposit and copper substrate were modeled using a regular Pearson VII function. The d-spacings were obtained from the profile fit. Lattice parameters were determined by least squares refinement, using reflections from the copper substrate as an internal standard.

Results and Discussion

Solutions of silver(I) were prepared in the Lewis acidic $AlCl_3$-EtMeImCl melts by the controlled-potential anodization of a silver electrode at an applied potential of 1.2 V. This method was simple and rapid and could be used to precisely control the silver(I) concentration. Sampled-current voltammograms constructed from chronoamperometric current-time transients recorded at a stationary platinum electrode in 5.00, 10.0, 15.0, 20.0, and 25.0 mmol L^{-1} solutions of silver(I) in the 66.7-33.3 mole percent (mol %) melt are shown in Fig. 1. These transients were obtained by stepping the electrode potential from an initial value of 2.0 V, where no faradaic reaction takes place, to the potential of interest; the current was sampled at 10 s following the application of each pulse. After the desired data were collected, the resulting electrodeposit was oxidized from the electrode surface by holding the electrode potential at 2.0 V until the oxidation current decayed to the background level. The complete sequence was repeated at another potential. Thus, each data point in Fig. 1 was obtained at a deposit-free electrode surface. All of the chronoamperometric transients exhibited Cottrell behavior; even those acquired in the potential region where silver(I) adsorption was observed (*vide infra*).

The voltammograms recorded in the 5.00 and 10.0 mmol L^{-1} solutions exhibit well defined limiting currents due to the mass-transport-limited reduction of silver(I) to silver metal[17]

$$Ag(I) + e^- \rightleftharpoons Ag(s) \quad [1]$$

However, at potentials proximate to 100 mV, the currents in these voltammograms increase above the limiting currents for the reduction of silver(I) due to the codeposition of aluminum with silver

$$xAg(I) + 4(1 - x)Al_2Cl_7^- + (3 - 2x)e^- \rightleftharpoons Ag_xAl_{1-x}(s) + 7(1 - x)AlCl_4^- \quad [2]$$

where $1 - x$ represents the atomic fraction of aluminum in the resulting Ag-Al alloy.

The three sampled-current voltammograms acquired in solutions where the silver(I) concentration was ≥15.0 mmol L^{-1} exhibit an obvious diminution in the current in the potential region extending from about 0.65 to 0.43 V, where the limiting current for the reduction of silver(I) should be observed. These current distortions were not especially reproducible. However, all three of these voltammograms do exhibit limiting currents in the 0.43 to 0.10 V potential region. Furthermore, these limiting currents scale linearly *vs.* the silver(I) concentration with the voltammograms recorded in the 5.00 and 10.0 mmol L^{-1} solutions.

Figure 2 shows cyclic-staircase voltammograms recorded in the same 10.0 and 25.0 mmol L^{-1} silver(I) solutions used to prepare Fig. 1. The voltammogram in Fig. 2a exhibits waves at 0.59 and 0.84 V due to the deposition and stripping of silver, respectively,[5] and another pair of waves centered slightly positive of 0 V due to the codeposition and stripping of aluminum from the electrodeposited alloy. The voltammogram recorded in the 25.0 mmol L^{-1} solution (Fig. 2b) also exhibits waves due to the deposition and stripping of silver. As expected, these waves are shifted to more positive potentials relative to those in Fig. 2a because of the increased silver(I) concentration. However, in Fig. 2b the peak reduction current divided by the silver(I) concentration, $i_p^c/C_{Ag(I)}$, is only ~60% of that for the voltammogram in Fig. 2a, indicating that the silver(I) reduction current is smaller in the 25.0 mmol L^{-1} solution than anticipated. Also apparent in Fig. 2b is a postwave at *ca*. 0.44 V. This postwave does not become obvious until the silver(I) concentration is equal to or exceeds ~15.0 mmol L^{-1}. The magnitude of this postwave is dependent on the electrode history, *i.e*., it is small during the first scan at a freshly polished electrode, but increases in magnitude along with a corresponding decrease in $i_p^c/C_{Ag(I)}$ for the primary silver(I) reduction wave if the electrode is scanned repeatedly or immersed for an appreciable time in a solution that is ≥15.0 mmol L^{-1} in silver(I).

Taken together, the sampled-current and cyclic-staircase voltammetry experiments suggest that silver(I) adsorbs strongly on platinum. Thus, the diminished currents seen in the voltammetric waves in Fig. 1 that were recorded in solutions containing ≥15.0 mmol L^{-1} silver(I) are due to the partial blocking of the active area of the electrode by the adsorbate. As a result of the extra stability imparted by the adsorption process, the adsorbed silver(I) is reduced at more negative potentials than the freely diffusing silver species. Thus, the expected value of the limiting current is not attained until the potential reaches about 0.43 V and the adsorbed silver(I) is reduced, restoring the full active area of the electrode. Furthermore, the presence of the postwave is consistent with the model for strong adsorption of the reactant (SAR) as described by Wopschall and Shain.[18]

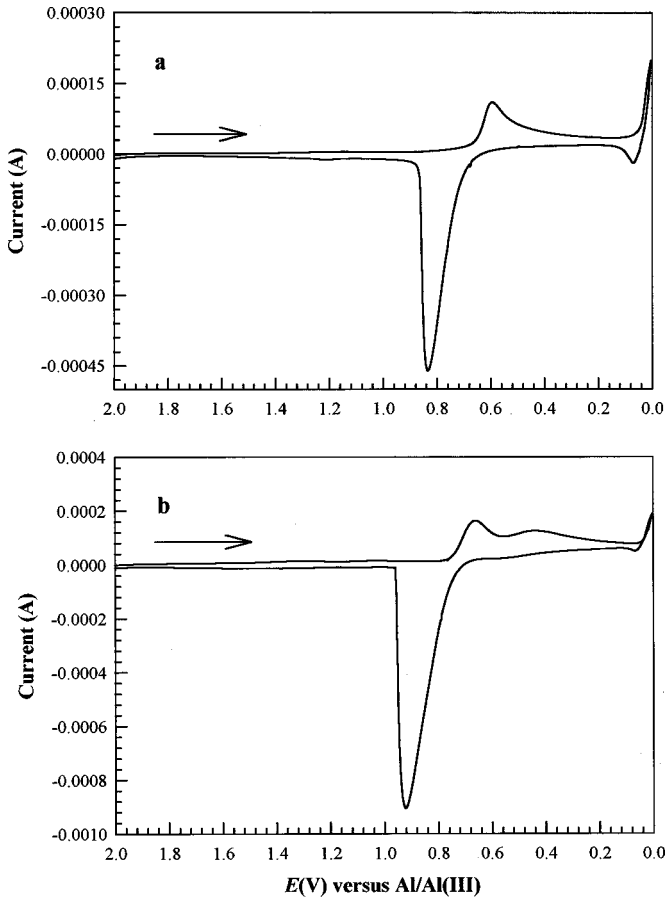

Figure 2. Cyclic-staircase voltammograms recorded at a stationary platinum electrode in the 66.7-33.3 mol % melt. The silver(I) concentrations were (a) 10.0 and (b) 25.0 mmol L^{-1}. The scan rate was 50 mV s^{-1}, and the step size was 1 mV.

Because the limiting currents in the 0.43 to 0.10 V potential region of the voltammograms in Fig. 1 scale linearly *vs*. the silver(I) concentration, the following equation can be used to estimate $1 - x$ in the Ag_xAl_{1-x} alloy from the voltammetric data recorded in the five solutions

$$1 - x = 1/\{1 + 3[i_l/(i_t - i_l)]\} \quad [3]$$

In this equation, i_l is the limiting current for the electrodeposition of pure silver and a measure of the partial current for silver deposition, i_t is the total current in the potential region where the codeposition of aluminum with silver is observed, and $i_t - i_l$ represents the partial current for silver deposition. The presence of a silver(I) adsorbate should not affect the alloy composition calculated from Eq. 3 because the current was sampled 10 s after the application of the potential step when the current is likely to be supported only by diffusion. That is, the reduction of the silver(I) adsorbate would be expected to take place rapidly after the application of a potential step with a final potential of 0.43 V or less, and the current component for this reduction process should decay to zero long before 10 s have elapsed.[19]

Figure 3 shows plots of $1 - x$ *vs*. *E* that were constructed from the sampled-current voltammograms in Fig. 1. These plots show that the atomic fraction of aluminum in the alloy is dependent on both the potential and the silver(I) concentration. As the applied potential approaches 0 V, which is the point at which the bulk deposition of aluminum is normally observed, the alloy composition tends to become independent of the silver(I) concentration. A similar result was found in the Co-Al system.[2] In addition, the data in Fig. 3 suggest

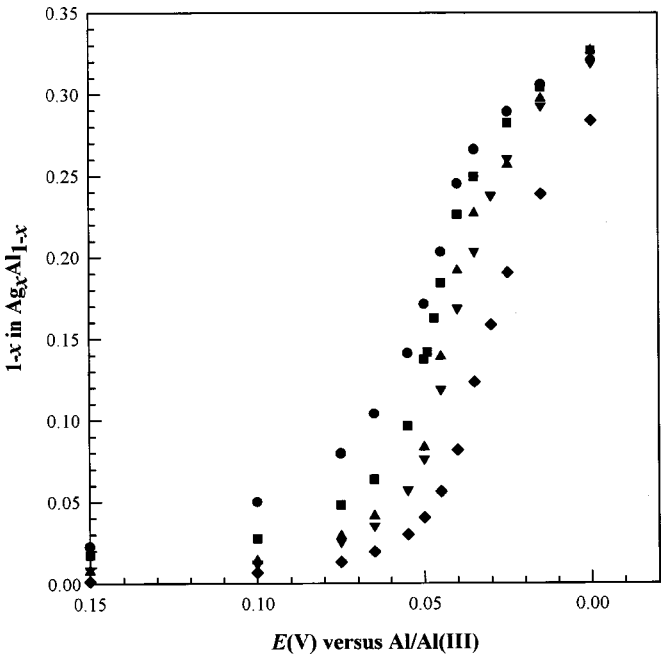

Figure 3. Atomic fraction of aluminum in the Ag-Al alloy, $1 - x$, as a function of potential based on the sampled-current voltammograms in Fig. 1. The silver(I) concentrations were (●) 5.00, (▲) 10.0, (■) 15.0, (▼) 20.0, and (◆) 25.0 mmol L^{-1}.

that in theory it should be possible to prepare bulk Ag-Al electrodeposits in the 66.7-33.3 mol % melt with an atomic fraction of aluminum approaching 0.33 if the silver(I) concentration is maintained below about 20 mmol L^{-1}. The concentration dependence of the alloy composition indicates that the aluminum codeposition process is kinetically limited, *i.e*., the partial current for the codeposition of aluminum lags behind that for silver as the latter increases with increasing silver(I) concentration. A similar dependence of the alloy composition on the transition metal concentration was noted during the electrodeposition of Co-Al[2] and Ni-Al[10], but not Cu-Al[5] in this same molten salt.

Dependence of the Ag-Al alloy composition on the melt composition.—$Al_2Cl_7^-$ is the principal reducible chloroaluminate species in the $AlCl_3$-EtMeImCl melt and must therefore participate in the mechanism of the reaction depicted in Eq. 2. (Small amounts of reducible $Al_3Cl_{10}^-$ may also be present in very acidic melt.[11]) By varying the composition of the melt, it is possible to alter the $Al_2Cl_7^-$ concentration and thereby probe the relationship between the $Al_2Cl_7^-$ concentration and the Ag-Al alloy composition. Figure 4 shows sampled-current voltammograms that were recorded in 5.00 and 25.0 mmol L^{-1} solutions of silver(I) in the 55.0-45.0, 60.0-40.0, and 66.7-33.3 mol % melts. The $Al_2Cl_7^-$ concentrations in these melts are 0.96, 1.95, and 3.36 mmol L^{-1}, respectively. Plots of $1 - x$ *vs*. E derived from the partial currents in Fig. 4 are shown in Fig. 5. They indicate that at a fixed silver(I) concentration, the Ag-Al alloy composition is dependent on the applied potential, but within the experimental error of these measurements, it displays little or no obvious or regular dependence on the $Al_2Cl_7^-$ concentration. From these results, we conclude that the Ag-Al electrode reaction depicted in Eq. 2 is probably pseudo-first-order in silver(I), *i.e*., the concentration of $Al_2Cl_7^-$ is so large relative to the silver(I) concentration that the kinetics of the reaction depend only on silver(I). This conclusion is supported by the fact that the $Al_2Cl_7^-$ concentration in the 55.0-45.0 mol % melt containing 25.0 mmol L^{-1} silver(I) is more than 38 times greater than the latter, and this ratio is even larger in the solutions prepared with the 60.0-40.0 and 66.7-33.3 mol % melts.

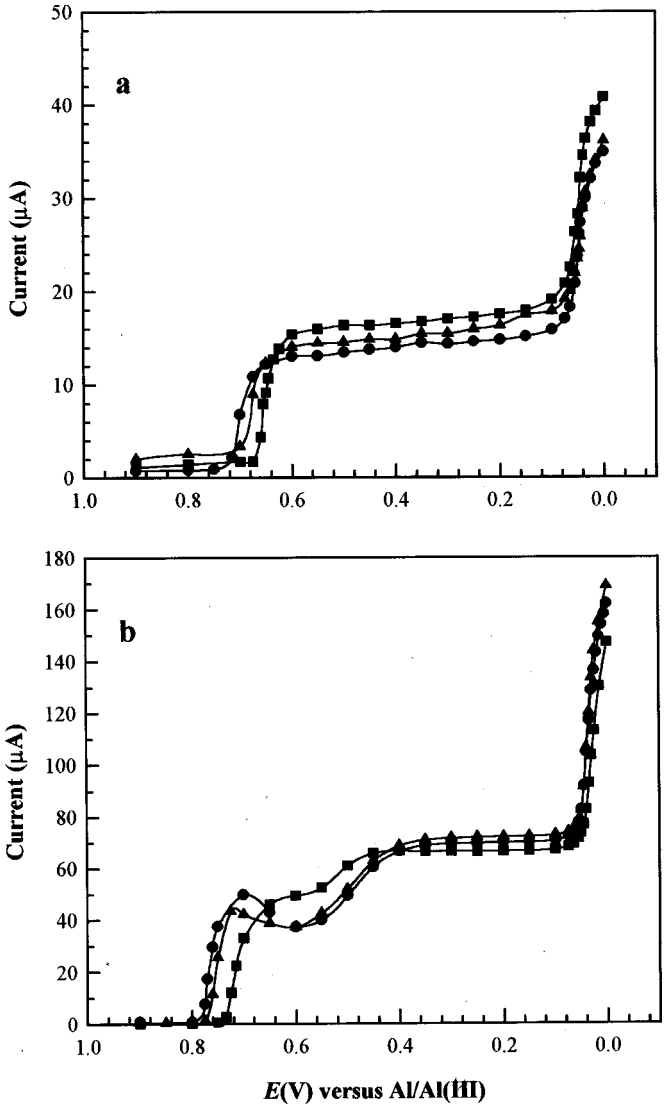

Figure 4. Sampled-current voltammograms recorded at a stationary platinum electrode in (a) 5.00 mmol L^{-1} and (b) 25.0 mmol L^{-1} solutions of silver(I): (■) 66.7-33.3, (▲) 60.0-40.0, and (●) 55.0-45.0 mol % melt. The current was sampled at 10 s.

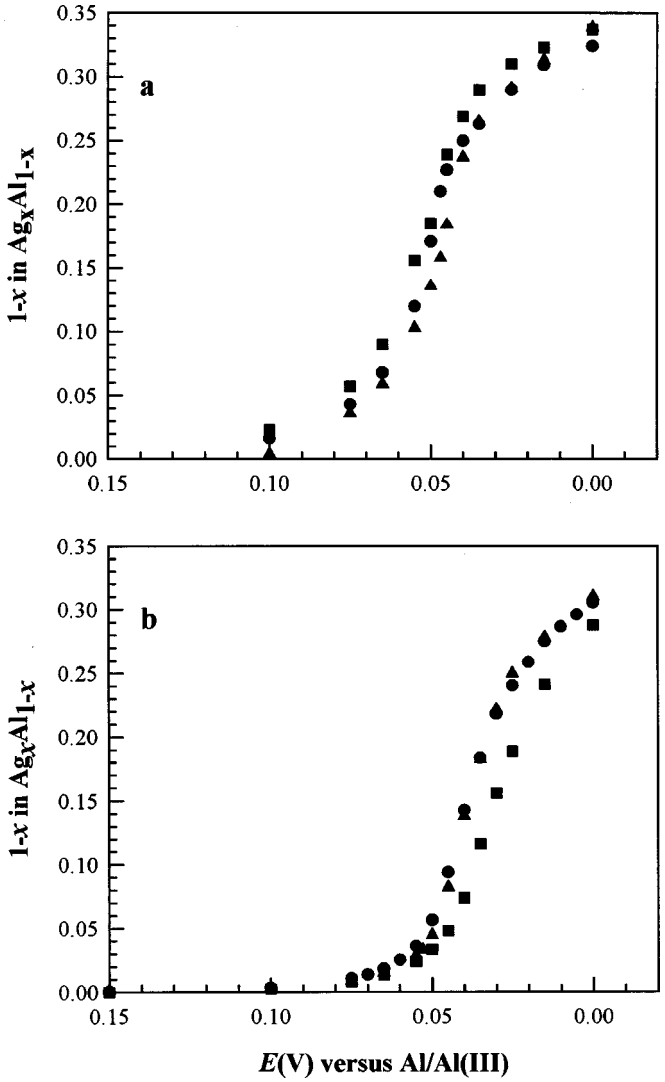

Figure 5. Atomic fraction of aluminum in the Ag-Al alloy, $1 - x$, as a function of potential based on the sampled-current voltammograms in (a) Fig. 4a and (b) Fig. 4b, (■) 66.7-33.3, (▲) 60.0-40.0, and (●) 55.0-45.0 mol % melt.

Electrodeposition of Ag-Al alloy at a tungsten electrode.—A sampled-current voltammogram was recorded at a tungsten electrode in a 25.0 mmol L^{-1} solution of silver(I) to determine if the adsorption phenomenon found at platinum also takes place at this electrode and to verify that the alloy composition is independent of the substrate material. The resulting voltammogram is shown in Fig. 6. Also shown for comparison is a voltammogram recorded at a platinum electrode in this same solution (Fig. 1). Like the latter, the voltammogram recorded at tungsten is distorted in the potential region where the limiting current for silver(I) reduction is normally expected to occur. However, in this case, not only is the current smaller than expected due to blocking of the electrode surface by the silver(I) adsorbate, but a substantial overpotential is needed to induce the nucleation of silver on the tungsten surface. Furthermore, the slow nucleation/growth of the silver deposit produces an artificial current maximum in the voltammogram at *ca*. 0.62 V. The slow nucleation kinetics at tungsten were confirmed by the potential-dependent maxima present in the current-time transients used to construct the voltammogram. Such phenomena were absent during potential-step experiments conducted at the platinum electrode. Slow nucleation/growth is routinely observed during the electrodeposition of metals on foreign substrates such as tungsten and glassy carbon from room-temperature chloroaluminate melts, but rarely encountered at platinum.[5,20] Figure 7 shows plots of $1 - x$ *vs*. E that were constructed from the partial currents in Fig. 6 using Eq. 3. These plots show that the alloy composition measured at tungsten is virtually indistinguishable from that determined at platinum, indicating that the Ag-Al alloy composition is independent of the substrate material.

Stability of the electrodeposited Ag-Al alloy.—Like the Co-Al, Cu-Al, Fe-Al, and Ni-Al alloy systems examined in previous studies, electrodeposited Ag-Al alloys are unstable in solutions containing the noble metal ion. That is, if the electrodeposited Ag-Al alloy is allowed to sit at open circuit in a solution of silver(I), the aluminum in the alloy will eventually be replaced by silver through a displacement reaction such as the following

$$Ag_xAl_{1-x}(s) + 3(1 - x)Ag(I) + 7(1 - x)AlCl_4^- \rightleftharpoons (3 - 2x)Ag(s) + 4(1 - x)Al_2Cl_7^- \quad [4]$$

The equilibrium constant for this reaction, K_{disp}, can be estimated

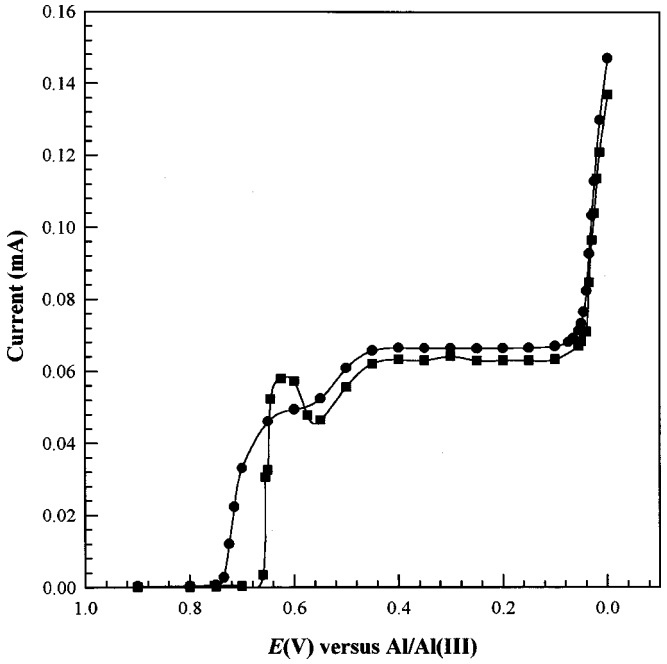

Figure 6. Sampled-current voltammograms recorded at stationary electrodes in a 25.0 mmol L^{-1} solution of silver(I) in the 66.7-33.3 mol % melt: (●) platinum and (■) tungsten. The current was sampled at 10 s.

from the formal potential of the Ag(I)/Ag electrode reaction, $E^{0\prime}_{Ag(I)/Ag}$, measured against the Al(III)/Al reference electrode, which is based on the reaction

$$4Al_2Cl_7^- + 3e^- \rightleftharpoons Al(s) + 7AlCl_4^- \qquad [5]$$

and is normally assigned $E^{0\prime}_{Al(III)/Al} = 0$ V, by using the familiar relationship

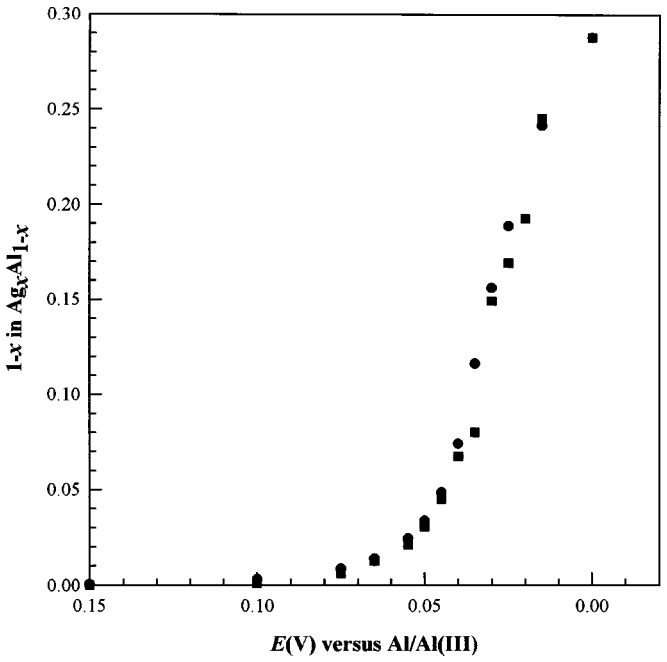

Figure 7. Atomic fraction of aluminum in the Ag-Al alloy, $1 - x$, as a function of potential based on the sampled-current voltammograms in Fig. 6: (●) platinum and (■) tungsten.

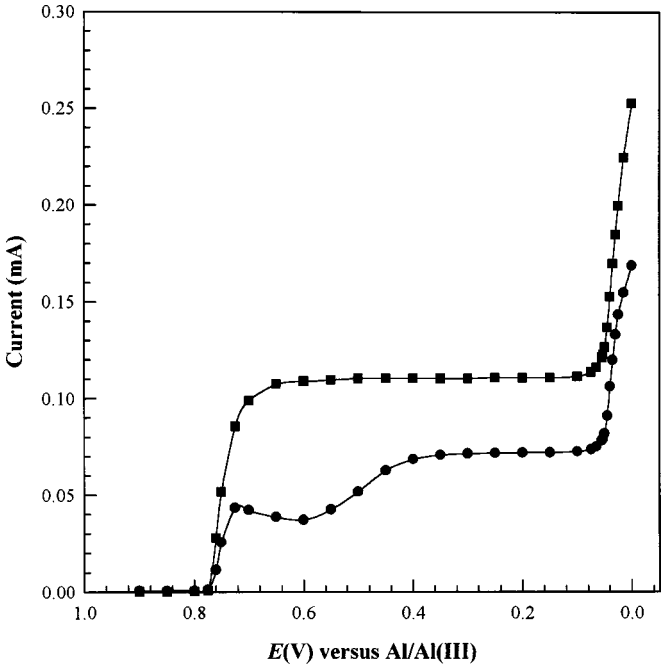

Figure 8. Sampled-current voltammograms recorded at a stationary platinum electrode in 25.0 mmol L^{-1} solutions of silver(I): (●) 60.0-40.0 mol % melt and (■) 60.0-40.0 mol % melt + 45.4% (v/v) benzene. The current was sampled at 10 s.

$$K_{disp} = \exp[(3F/RT)(E^{0\prime}_{Ag(I)/Ag} - E^{0\prime}_{Al(III)/Al})] \qquad [6]$$

The required values of $E^{0\prime}_{Ag(I)/Ag}$ were determined by constructing Nernst plots from equilibrium potential data recorded as a function of the silver(I) concentration during the controlled-potential anodization of silver electrodes in the three melts described above. These Nernst plots were linear ($R^2 = 0.999 \pm 0.001$), and the slopes of these plots gave $n = 1.0 \pm 0.1$. The intercepts yielded $E^{0\prime}_{Ag(I)/Ag}$ values of 0.881 ± 0.001, 0.877 ± 0.001, and 0.844 ± 0.001 V in the 55.0-45.0, 60.0-40.0, and 66.7-33.3 mol % melts, respectively. From the average value of $E^{0\prime}_{Ag(I)/Ag}$, K_{disp} is estimated to be about 1×10^{44} at 298 K. Although the rate of the process in Eq. 4 is not known, this approximate calculation nevertheless serves to illustrate the substantial thermodynamic driving force for this displacement reaction. As a result of this reaction, the composition of actual bulk Ag-Al alloy electrodeposits may differ substantially from the predictions of potential *vs*. composition diagrams based on partial currents such as those shown in Fig. 3 and elsewhere in this article. This is because there are unavoidable periods of time during the preparation and handling of bulk electrodeposits when they have been removed from cathodic protection, but are still in contact with melt containing silver(I).

Effect of benzene cosolvent on the Ag-Al alloy electrodeposition process.—In previous investigations, it was found that the quality of bulk electrodeposits prepared from acidic $AlCl_3$-EtMeImCl could sometimes be improved by the addition of a cosolvent such as benzene to the melt.[10,21] Figure 8 shows a sampled-current voltammogram that was recorded at a platinum electrode in 60.0-40.0 mol % melt containing 45.4% (vol %) benzene as a cosolvent. The silver(I) concentration in this admixture was 25.0 mmol L^{-1}. Shown for comparison is a voltammogram recorded at the same electrode in a 25.0 mmol L^{-1} solution of silver(I) in neat 60.0-40.0 mol % melt.

The addition of benzene to the melt has a twofold effect. First, it lowers the viscosity of the molten salt, increasing the diffusion coefficient of silver(I) from $(7.2 \pm 0.2) \times 10^{-7}$ $cm^2\ s^{-1}$ in neat

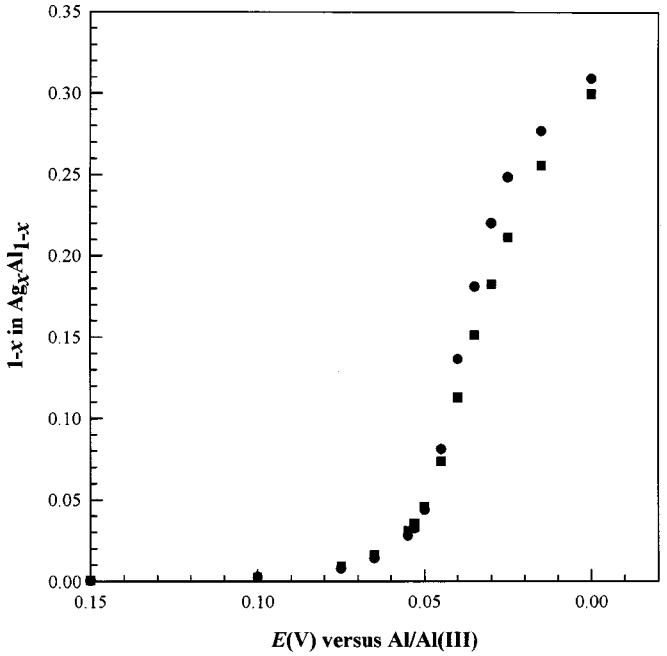

Figure 9. Atomic fraction of aluminum in the Ag-Al alloy, $1 - x$, as a function of potential based on the sampled-current voltammograms in Fig. 8: (●) 60.0-40.0 mol % melt and (■) 60.0-40.0 mol % melt + 45.4% (v/v) benzene.

60.0-40.0 mol % melt to $(17.1 \pm 0.1) \times 10^{-7}$ cm^2 s^{-1} in the mixture described above. Second, the added benzene inhibits the strong adsorption of silver(I) on the platinum electrode, resulting in a sampled-current voltammogram without the distortions seen at the same silver(I) concentration in neat melt. Surprisingly, the addition of benzene has very little effect on the alloy composition, as illustrated by the plot of $1 - x$ *vs.* E shown in Fig. 9. This indicates that the rate of the aluminum codeposition process increases commensurately with the increase in the limiting current for silver(I) reduction when the melt viscosity is lowered by the addition of benzene.

Preparation and analysis of bulk Ag-Al electrodeposits.—Bulk Ag-Al alloys were electrodeposited under galvanostatic conditions onto 2.54 cm lengths of 0.75 mm diam copper wire from 25.0 mmol L^{-1} solutions of silver(I) in the 60.0-40.0 mol % melt containing 45.4 vol % benzene. It was necessary to use melt/benzene mixtures to prepare bulk deposits because deposits prepared in pure melt contained trapped melt, and they deteriorated rapidly upon exposure to the atmosphere. Four different current densities were used for these deposition experiments: 1.7×10^{-3}, 3.3×10^{-3}, 5.0×10^{-3}, and 6.7×10^{-3} A cm^{-2}. In each case, the current was continued until a deposition charge of about 17 C had been attained, which corresponds to a 20 μm thick film based on pure silver. All of the electrodeposits examined by EDS showed characteristic X-rays for silver or silver in combination with aluminum. No chlorine (as chloride) was detected in any of the deposits. Alloy compositions were determined from semiquantitative analysis of the EDS data, and the results are shown in Table I. Deposition current densities of 1.7×10^{-3} A cm^{-2} or less resulted in pure silver films. As the current density was increased, the aluminum content increased. The highest aluminum content found in the bulk films by using EDS was

Table I. Aluminum composition (EDS, semiquantitative) as a function of deposition current density.

Current density (A cm^{-2})	Atomic fraction of aluminum
1.7×10^{-3}	0
3.3×10^{-3}	0.069
5.0×10^{-3}	0.122
6.7×10^{-3}	0.113

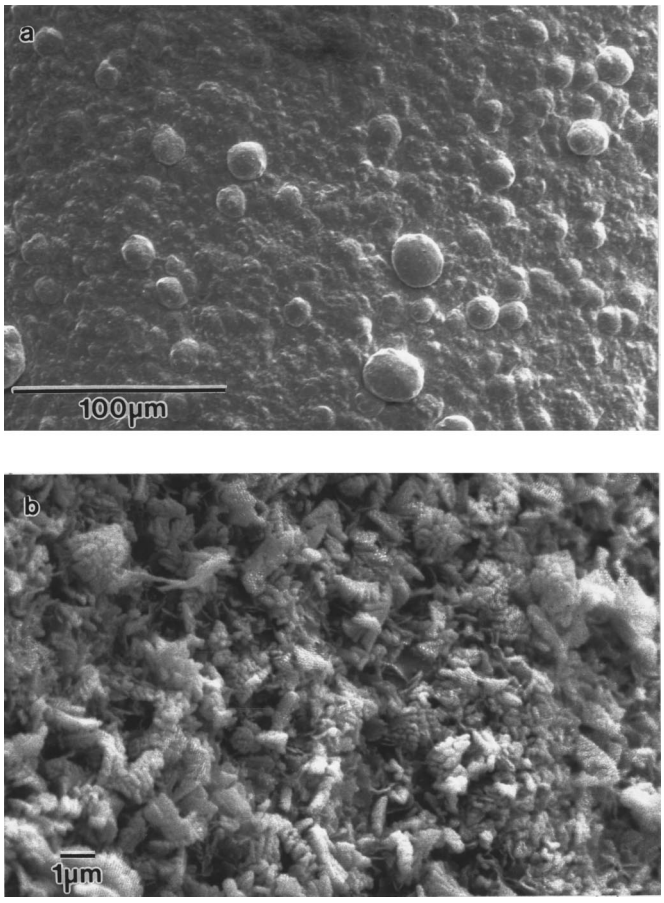

Figure 10. SEM micrographs of silver and silver aluminum alloys electrodeposited at 25°C from a 25.0 mmol L^{-1} solution of silver(I) in the 60.0-40.0 mol % melt + 45.4% (v/v) benzene. The deposition current densities were (a) 1.7×10^{-3} and (b) 5.0×10^{-3} A cm^{-2}.

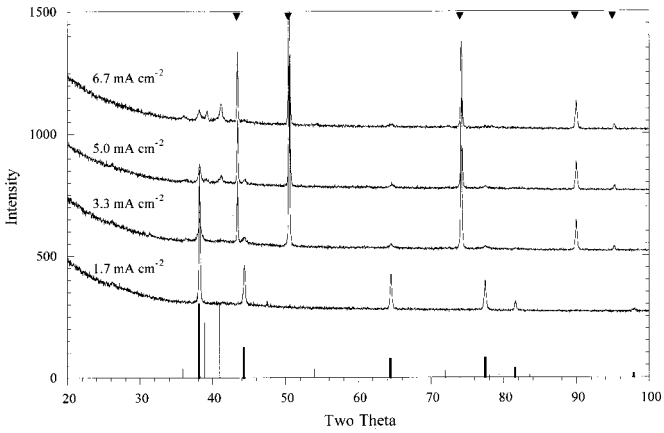

Figure 11. XRD patterns (Cu Kα) of silver and silver-aluminum alloys electrodeposited at 25°C from a 25.0 mmol L^{-1} solution of silver(I) in the 60.0-40.0 mol % melt + 45.4% (v/v) benzene. The vertical lines rising from the x axis represent the reflections for fcc silver[27] and δ-Ag$_2$Al.[26] The triangles at the top of the figure represent the reflections due to the copper substrate.

Table II. Ag and Ag_2Al lattice parameters as a function of deposition current density.

Current density (A cm^{-2})	Lattice parameters (JCPDS)[22,23] Ag (4.0862 Å)	Ag_2Al (*a*) (2.8779 Å)	Ag_2Al (*c*) (4.6225 Å)
1.7×10^{-3}	4.0827 ± 0.0008		
3.3×10^{-3}	4.0850 ± 0.0008		
5.0×10^{-3}	4.084 ± 0.002	2.875 ± 0.007	4.62 ± 0.01
6.7×10^{-3}	4.084 ± 0.002	2.882 ± 0.003	4.602 ± 0.005

0.122 atom %. The morphologies of the silver and silver-aluminum alloy electrodeposits are shown in Fig. 10. The pure silver deposits (Fig. 10a) are dense and compact, whereas the deposit containing 0.122 atomic fraction aluminum has a porous, somewhat dendritic structure (Fig. 10b).

Deposit structure and morphology.—The X-ray patterns of the films listed in Table I are shown in Fig. 11. The pure silver film that was deposited at 1.7×10^{-3} A cm^{-2} is single phase and has a face-centered cubic (fcc) structure. The film is dense and thick enough so that the reflections from the copper substrate do not appear in the diffraction pattern. As the current density is increased, the intensity of the fcc Ag reflections begins to decrease. Reflections that can be indexed to hcp (hexagonal close-packed) δ-Ag_2Al also begin to appear in the diffraction patterns. In addition to these microstructural features, reflections from the copper substrate are visible in films deposited at higher current densities. This implies that the deposits become thinner or that the average atomic weight is reduced as the current density is increased. Both of these factors may become important as aluminum is incorporated into deposits of equal charge density.

The maximum solubility of aluminum in fcc silver is about 0.204 atom % at 450°C.[22] The solubility is reduced to about 0.07 atom % at room temperature. One would expect the lattice parameter of the solid solution to decrease only slightly as aluminum alloys substitutionally with silver because aluminum and silver atoms are essentially the same size. The reported decrease in lattice parameter from that of pure silver to that of the solid solution containing 0.204 atom % aluminum is only 2.3×10^{-3} nm.[23-25]

The fcc Ag and hcp δ-Ag_2Al lattice parameters obtained from the XRD data are listed as a function of deposition current density in Table II. The two lattice parameters measured for the hcp δ-Ag_2Al phase are nearly the same within experimental error as the JCPDS values.[26] The fcc Ag lattice parameters for all of the deposits are slightly less (2.2×10^{-4} to 3.5×10^{-4} nm) than the accepted JCPDS value for silver,[27] indicating that the maximum aluminum content of the fcc phase is less than 0.03 atomic fraction. In addition, there does not appear to be the systematic change in the lattice parameters with current density one would expect if aluminum were to alloy substitutionally into the silver lattice. The data suggest that as the aluminum content of the alloy increases, the amount of δ-Ag_2Al in the deposit increases whereas the aluminum composition of the fcc silver solid solution remains low and essentially constant.

Acknowledgment

This research was supported by Air Force Office of Scientific Research grant no. F49620-00-1-0123.

The University of Mississippi assisted in meeting the publication costs of this article.

References

1. R. T. Carlin, P. C. Trulove, and H. C. De Long, *J. Electrochem. Soc.*, **143**, 2747 (1996).
2. J. A. Mitchell, W. R. Pitner, C. L. Hussey, and G. R. Stafford, *J. Electrochem. Soc.*, **143**, 3448 (1996).
3. M. R. Ali, A. Nishikata, and T. Tsuru, *Electrochim. Acta*, **42**, 2347 (1997).
4. T. P. Moffat, *J. Electrochem. Soc.*, **141**, L115 (1994).
5. B. J. Tierney, W. R. Pitner, J. A. Mitchell, C. L. Hussey, and G. R. Stafford, *J. Electrochem. Soc.*, **145**, 3110 (1998).
6. J. A. Mitchell, Ph.D. Dissertation, University of Mississippi, University, MS (1997).
7. G. R. Stafford, *J. Electrochem. Soc.*, **136**, 635 (1989).
8. T. P. Moffat, G. R. Stafford, and D. E. Hall, *J. Electrochem. Soc.*, **140**, 2779 (1993).
9. T. P. Moffat, *J. Electrochem. Soc.*, **141**, 3059 (1994).
10. W. R. Pitner, C. L. Hussey, and G. R. Stafford, *J. Electrochem. Soc.*, **143**, 130 (1996).
11. C. L. Hussey, in *Chemistry of Nonaqueous Solutions*, G. Mamantov and A. I. Popov, Editors, p. 227, VCH Publishers, New York (1994).
12. R. D. Blue and F. C. Mathers, *Trans. Electrochem. Soc.*, **69**, 529 (1936).
13. J. S. Wilkes, J. A. Levisky, R. A. Wilson, and C. L. Hussey, *Inorg. Chem.*, **21**, 1263 (1982).
14. M. A. M. Noel, P. C. Trulove, and R. A. Osteryoung, *Ann. Chem.*, **63**, 2892 (1991).
15. C. L. Hussey and X. Xu, *J. Electrochem. Soc.*, **138**, 1886 (1991).
16. T. B. Scheffler and C. L. Hussey, *Inorg. Chem.*, **23**, 1926 (1984).
17. X. H. Xu and C. L. Hussey, *J. Electrochem. Soc.*, **139**, 1295 (1992).
18. R. H. Wopschall and I. Shain, *Anal. Chem.*, **39**, 1514 (1967).
19. J. H. Christie, R. A. Osteryoung, and F. C. Anson, *J. Electroanal. Chem.*, **13**, 236 (1967).
20. X-H. Xu and C. L. Hussey, *J. Electrochem. Soc.*, **140**, 1226 (1993).
21. Q. Liao, W. R. Pitner, G. Stewart, C. L. Hussey, and G. R. Stafford, *J. Electrochem. Soc.*, **144**, 936 (1997).
22. *Binary Alloy Phase Diagrams*, T. B. Massalski, Editor, American Society for Metals, Metals Park, OH (1986).
23. A. F. Westgren and A. J. Bradley, *Philos. Mag.*, **6**, 280 (1928).
24. C. S. Barrett, *Metals Alloys*, **4**, 63 (1933).
25. F. Foote and E. R. Jette, *Trans. AIME*, **143**, 151 (1941).
26. Card No. 14-647, International Center for Diffraction Data, Newtown, PA.
27. Card No. 4-783, International Center for Diffraction Data, Newtown, PA.